Effect of open-core screw dislocation on axial conductivity in semiconductor crystals

Hisao Taira[*] and Motohiro Sato

Division of Engineering and Policy for Sustainable Environment, Faculty of Engineering, Hokkaido University, Kita 13 Nishi 8, Kita-ku, Sapporo 060-8628, Japan

Abstract.   The alternating current (AC) conductivity in semiconductor crystals with an open-core screw dislocation is studied in the current work. The screw dislocation in crystalline media results in an effective potential field which affects the electronic transport properties of the system. Therefore, from a technological view point, it is interesting to investigate properties of AC conductivity at frequencies of a few terahertz. To quantify the screw-induced potential effect, we calculated the AC conductivity of dislocated crystals using the Kubo formula. The conductivity showed peaks within the terahertz frequency region, where the amplitude of the AC conductivity was large enough to be measured in experiments. The measurable conductivity peaks did not arise in dislocation-free crystals threaded by a magnetic flux tube. These results imply different conductivity mechanisms in crystals with a screw dislocation than those threaded by a magnetic flux tube, despite the apparent similarity in their electronic eigenstates.

Keywords: alternating conductivity; screw dislocation; electronic structure; quantum phase; numerical calculation

1. Introduction

The void associated with a screw dislocation core modulates electronic states. This open-core screw dislocation has been found in semiconductors such as silicon carbide (SiC) (Si *et al.* 1997, Vetter and Dudley 2002, Dudley *et al.* 2003, Ma 2006). In order to investigate the electronic structure of such systems, considerable attention has been focused on comparing the wave propagation phenomena in the single-screw dislocated, three-dimensional crystal system and in the Aharonov-Bohm (AB) system (Carvalho *et al.* 2007, Turski *et al.* 2007, Netto and Furtado 2008, Turski and Mińkowski 2009). A quantum effect on electrons moving in the screw-dislocated system is mainly given by the phase shift of the wave functions (Kawamura 1978, Araki *et al.* 1981, Bausch and Schmitz 1998, Bausch *et al.* 1999, Look and Sizelove 1999, Furtado *et al.* 2001, Bakke and Moraes 2012). This phase shift occurs even if the electrons' wave functions do not touch the screw dislocation. This phenomenon is reminiscent of the AB effect since electrons in the AB system also exhibit a quantum phase shift despite the fact that electrons do not touch the magnetic field (Aharonov and Bohm 1959). These two observations indicate that the magnetic field mimics the screw

---

dislocation. Experimental measurements have shown these characteristics (Schafler *et al.* 2001, Dumiszewska *et al.* 2007, Gilbert *et al.* 2011); however, there have been very few efforts to develop a comprehensive theoretical model to investigate the effect of the screw dislocation on physical quantities. Calculating the alternating current (AC) conductivity is a powerful tool to investigate the effect of the screw dislocation since it provides information on both the momentum and energy spectrum.

In this paper, we numerically calculate the AC conductivity of the screw-dislocated system. This same calculation has been performed in the AB system. The most important difference is that AC conductivity is measurable in the screw-dislocated system but is not measurable in the AB system. This result provides evidence that the quantum phase shifts induced by the screw-dislocated system and the AB system contribute to the AC conductivity in different ways. Understanding the mechanisms of this difference sheds new light for further exploration of new phenomena based on screw-dislocated systems.

2. Model and method

2.1 Mathematical preliminary

First, we derive the Schrödinger equation, which describes the electronic states of a crystal of simple cubic structure with a hollow screw dislocation (Kawamura 1978). We assume that the Burgers vector is given by $\boldsymbol{b} = b\boldsymbol{e}_z$, where b is a constant, which determines the spatial distribution, amplitude and direction of the screw dislocations (Fig. 1).

In the tight-binding scenario, the electronic wave function $C(\boldsymbol{n})$ at site $\boldsymbol{n}$ satisfies the relation,

$$EC(\boldsymbol{n}) - T \sum_{i=1}^{6} C(\boldsymbol{n} + \boldsymbol{a}_i) = 0, \tag{1}$$
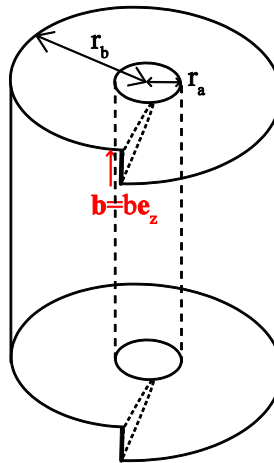

Fig. 1 Schematic view of the three-dimensional system with a single hollow screw dislocation

where E and T are the on-site energy and transfer-matrix between two neighboring sites, respectively, and $n + a_i$ $(i = 1, ..., 6)$ are the nearest neighbor sites of n.

In our model, the site-dependence of T is ignored since we are focusing on the topological nature of the effect of screw dislocation on electronic structure, at this stage.

To find the spatial dependence of a_i, we set a_i as follows

$$a_1 = ae_x + af(r,\theta)e_z = -a_2, \tag{2}$$

$$a_3 = ae_y + ag(r,\theta)e_z = -a_4, \tag{3}$$

$$a_5 = ae_z = -a_6, \tag{4}$$

where $e_j, (j = x, y, z)$ are unit vectors in the direction of the j-axis represented by Descartes coordinates. a is a lattice constant of the system and $f(r,\theta)$ and $g(r,\theta)$ are functions represented by polar coordinates which determine the lattice shape. By imposing the condition that a cubic structure of the system contains a single screw dislocation in the direction of the z axis, e_z satisfies the relation

$$\int_0^{2\pi} e_\theta \, r d\theta = be_z, \tag{5}$$

where

$$e_\theta = -\sin\theta \, a_1 + \cos\theta \, a_3 \tag{6}$$

is the tangential unit vector of a spiral curve (i.e., parallel to the θ direction), which lies on a single lattice plane since the amplitude of the Burgers vector b is much smaller compared to the size of the system. Eqs. (2), (3), and (5) lead to function forms of $f(r,\theta)$ and $g(r,\theta)$

$$f(r,\theta) = -\frac{\sin\theta}{2\pi r}, \tag{7}$$

$$g(r,\theta) = \frac{\cos\theta}{2\pi r}. \tag{8}$$

We have now derived the function forms of a_i.

2.2 Schrödinger equation

To derive the expression of continuum approximation of Eq. (1), we expand the function $C(n + a_i)$ in the Taylor series with respect to a_i up to the second order

$$C(x + a_{ix}, y + a_{iy}, z + a_{iz}) \sim \sum_{n=0}^{2} \frac{1}{n!}\left(a_{ix}\frac{\partial}{\partial x} + a_{iy}\frac{\partial}{\partial y} + a_{iz}\frac{\partial}{\partial z}\right)^n C(x,y,z)$$

$$= C(x,y,z) + \left(a_{ix}\frac{\partial}{\partial x} + a_{iz}\frac{\partial}{\partial z}\right)C(x,y,z)$$

$$+ \frac{1}{2!}\left(\frac{\partial^2}{\partial x^2} + a_{iz}^2\frac{\partial^2}{\partial z^2} + \frac{\partial a_{iz}}{\partial x}\frac{\partial}{\partial z} + 2a_{iz}\frac{\partial^2}{\partial x \partial z}\right)C(x,y,z), \tag{9}$$

where a_{ij} are j components of a_i. The relations $a_1 = -a_2$, $a_3 = -a_4$, $a_5 = -a_6$ in Eqs. (2), (3) and (4) lead to the explicit expression of the continuum limit of $\sum_{i=1}^{6} C(n + a_i)$ in Eq. (1)

$$\sum_{i=1}^{6} C(\boldsymbol{n} + \boldsymbol{a_i}) \sim 6C(\boldsymbol{r}) + \left[\frac{\partial^2}{\partial x^2} + \frac{\partial^2}{\partial y^2} + (2a_{1z}{}^2 + 1)\frac{\partial^2}{\partial z^2} + 2a_{1z}\frac{\partial^2}{\partial x \partial z} \right.$$
$$\left. + 2a_{2z}\frac{\partial^2}{\partial y \partial z} + \left(\frac{\partial a_{1z}}{\partial x} + \frac{\partial a_{2z}}{\partial y} \right)\frac{\partial}{\partial z} \right] C(\boldsymbol{r}). \tag{10}$$

Here, we use the symbol of position vector $\boldsymbol{r} = (r, \theta, z)$ instead of $\boldsymbol{n}$ since we are using a continuum description. Coordinate transformation from the Descartes coordinate system to polar coordinate system results in

$$\sum_{i=1}^{6} C(\boldsymbol{n} + \boldsymbol{a_i}) \sim 6C(\boldsymbol{r}) + \left[\frac{\partial^2}{\partial r^2} + \frac{1}{r}\frac{\partial}{\partial r} + \frac{1}{r^2}\left(\frac{\partial}{\partial \theta} + \frac{b}{2\pi}\frac{\partial}{\partial z} \right)^2 + \frac{\partial^2}{\partial z^2} \right] C(\boldsymbol{r}), \tag{11}$$

where we used Eqs. (7) and (8). The Schrödinger equation in the continuum approximation, in terms of cylindrical coordinates, is given by

$$(E - 6T)C(\boldsymbol{r}) - T\left[\frac{\partial^2}{\partial r^2} + \frac{1}{r}\frac{\partial}{\partial r} + \frac{1}{r^2}\left(\frac{\partial}{\partial \theta} + \frac{b}{2\pi}\frac{\partial}{\partial z} \right)^2 + \frac{\partial^2}{\partial z^2} \right] C(\boldsymbol{r}) = 0. \tag{12}$$

The spatial dependence of the transfer energy $T = T(\boldsymbol{r})$ results in (Bilby *et al.* 1955, Bausch *et al.* 1998, Bausch *et al.* 1999a, b)

$$-\frac{\hbar^2}{2m^*}\left\{ \frac{\partial^2}{\partial r^2} + \frac{1}{r}\frac{\partial}{\partial r} + \frac{1}{r^2}\left(\frac{\partial}{\partial \theta} + \frac{b}{2\pi}\frac{\partial}{\partial z} \right)^2 + \frac{\partial^2}{\partial z^2} + \frac{b^2}{2\pi^2 a^2 r^2}\left[1 + \frac{1}{2}\left(a\frac{\partial}{\partial z} \right)^2 \right] \right\} C(\boldsymbol{r}) = EC(\boldsymbol{r}), \tag{13}$$

where T is interpreted as $\hbar^2 / (2m^*)$.

It should be emphasized that the expression in Eq. (13) signifies the existence of the effective vector potential $\boldsymbol{A}^{\text{eff}}$ whose definition is given by

$$\boldsymbol{A}^{\text{eff}} = \boldsymbol{e}_\theta \frac{\hbar b}{2\pi r}\frac{\partial}{\partial z}. \tag{14}$$

The mathematical properties of $\boldsymbol{A}^{\text{eff}}$ are shown to be $\nabla \times \boldsymbol{A}^{\text{eff}} = \boldsymbol{0}$ and $\boldsymbol{A}^{\text{eff}} \propto \boldsymbol{e}_\theta/\text{r}$, and its properties mimic those of a vector, not effective, potential $\boldsymbol{A}$. This analogy reminds us that the magnitude of the Burgers vector b plays a similar role in the magnetic field. In fact, the electrons moving in the screw-dislocated system and the AB system have the same qualitative energy spectrum (Azevedo and Moraes 1998, Azevedo and Pereira 2000). Despite this similarity, $\boldsymbol{A}^{\text{eff}}$ and $\boldsymbol{A}$ contribute to the pronounced differences in the behavior of the dynamic conductivity of these two systems, since $\boldsymbol{A}^{\text{eff}}$ is a differential operator while $\boldsymbol{A}$ is not. This difference will be expanded on in Section 3.

2.3 The solution of the Schrödinger equation

In this subsection, we find the solution of the differential equation given in Eq. (13) by following Furtado *et al.* (2001). We assume the solution of Eq. (13) in separation variables form

$$C(\boldsymbol{r}) = R(r)e^{im\theta}e^{ik_z z}, \tag{15}$$

where m is the quantum number of the angular momentum of the electron, and k_z is the wave

number of the electron in the direction of z. Substituting Eq. (15) into Eq. (13), we obtain the one-dimensional Schrödinger equation

$$\left(\frac{d^2}{dr^2} + \frac{1}{r}\frac{d}{dr} + k^2 - \frac{v^2}{r^2}\right)R(r) = ER(r),\tag{16}$$

where

$$k^2 = \frac{2m^*E}{\hbar^2} - k_z{}^2,\tag{17}$$

$$v^2 = \left(m + \frac{k_z b}{2\pi}\right)^2 + \frac{b^2}{2\pi^2 a^2}\left(1 - \frac{k_z{}^2 a^2}{2}\right).\tag{18}$$

Since Eq. (16) is a Bessel differential equation, its general solution is given by

$$R(r) = B_1 J_v(kr) + B_2 N_v(kr),\tag{19}$$

where B_1 and B_2 are constants of integration, which can be numerically determined by the normalization condition of $J_v(kr)$ and $N_v(kr)$. Assigning the boundary condition of

$$R(kr_a) = R(kr_b) = 0,\tag{20}$$

Eq. (19) results in

$$J_v(kr_b)N_v(kr_a) - N_v(kr_b)J_v(kr_a) = 0.\tag{21}$$

Explicit forms of eigenfunctions can be obtained if the conditions of $kr_a \gg 1$ and $kr_b \gg 1$ are satisfied. Under these approximations, asymptotic forms of J_v and N_v with fixed v are given by (Furtado *et al.* 2001)

$$J_v(kr_a) \sim \sqrt{\frac{2}{\pi kr_a}}\left[\cos\left(kr_a - \frac{\pi v}{2} - \frac{\pi}{4}\right) - \frac{4v^2 - 1}{8kr_a}\sin\left(kr_a - \frac{\pi v}{2} - \frac{\pi}{4}\right)\right],\tag{22}$$

$$N_v(kr_a) \sim \sqrt{\frac{2}{\pi kr_a}}\left[\sin\left(kr_a - \frac{\pi v}{2} - \frac{\pi}{4}\right) + \frac{4v^2 - 1}{8kr_a}\cos\left(kr_a - \frac{\pi v}{2} - \frac{\pi}{4}\right)\right],\tag{23}$$

$$J_v(kr_b) \sim \sqrt{\frac{2}{\pi kr_b}}\left[\cos\left(kr_b - \frac{\pi v}{2} - \frac{\pi}{4}\right) - \frac{4v^2 - 1}{8kr_b}\sin\left(kr_b - \frac{\pi v}{2} - \frac{\pi}{4}\right)\right],\tag{24}$$

$$N_v(kr_b) \sim \sqrt{\frac{2}{\pi kr_b}}\left[\sin\left(kr_b - \frac{\pi v}{2} - \frac{\pi}{4}\right) + \frac{4v^2 - 1}{8kr_b}\cos\left(kr_b - \frac{\pi v}{2} - \frac{\pi}{4}\right)\right].\tag{25}$$

Substituting Eqs. (22)-(25) into Eq. (21), the explicit form of k is found to be

$$k^2 \sim \left(\frac{n\pi}{r_b - r_a}\right)^2 + \frac{v^2}{4r_b r_a},\tag{26}$$

where $n = 1,2,3,\cdots$ is the quantum number that indicates the oscillating modes in the range of $[r_a, r_b]$. Then, the eigenenergy E is given by

$$E = \frac{\hbar^2 k_z^2}{2m^*} + \frac{\hbar^2}{2m^*}\left[\left(\frac{n\pi}{r_b - r_a}\right)^2 + \frac{v^2}{4r_b r_a}\right]. \tag{27}$$

It should be noted that even though electrons do not touch the screw dislocation, v depends on b according to Eq. (18), indicating that E depends on b. This is the analogue of the AB effect noted in the Introduction.

3. Alternating current conductivity

The alternating current (AC) conductivity of the screw-dislocated system is derived in this section. According to the Kubo formula (Kubo 1957), the real part of the AC conductivity is expressed by

$$\sigma_{jj'}(\omega) = \frac{\pi}{V\omega} \sum_{\alpha,\alpha'} \langle \alpha|I_j|\alpha'\rangle\langle \alpha'|I_{j'}|\alpha\rangle \delta(E_\alpha - E_{\alpha'} - \hbar\omega), \tag{28}$$

where V is the volume of the system, ω is the angular frequency of the external electric field, $\hbar$ is the Planck constant, and j and j' are x, y, z-components. $\delta(\cdots)$ is the Dirac delta function, α and α' denote the quantum number of electrons, and I_j and $I_{j'}$ are current operators with j and j' components, respectively. Given the Hamiltonian H and eigenenergies E_α and $E_{\alpha'}$, $|\alpha\rangle$ and $|\alpha'\rangle$ represent the corresponding eigenstates, which satisfies the relations $H|\alpha\rangle = E_\alpha|\alpha\rangle$ and $H|\alpha'\rangle = E_{\alpha'}|\alpha'\rangle$, respectively. An explicit form of the current operator reads as

$$I_j = \frac{e}{m^*}\left(-i\hbar\frac{\partial}{\partial j} - A_j^{\text{eff}}\right), \tag{29}$$

where A_j^{eff} is the j-component of $\boldsymbol{A}^{\text{eff}}$.

From the rotational symmetry around the z-axis, off-diagonal components vanish from the conductivity and $\sigma_{xx}(\omega) = \sigma_{yy}(\omega) \neq \sigma_{zz}(\omega)$ is satisfied. Since $\boldsymbol{A}^{\text{eff}}$ is parallel to the direction of $\boldsymbol{e}_\theta$, $\boldsymbol{A}^{\text{eff}}$ affects the xx and yy components of the AC conductivity. Then, we concentrate on calculating $\sigma_{xx}(\omega) = \sigma_{yy}(\omega) \equiv \sigma(\omega)$. Since $|\alpha\rangle$ corresponds to the eigenfunctions given in Eq. (15) in our system, $\sigma(\omega) = \sigma_{v_+}(\omega) + \sigma_{v_-}(\omega)$ is obtained by substituting Eq. (15) and Eq. (29) into Eq. (28)

$$\sigma_{v_\pm}(\omega) = \frac{\pi e^2}{Vm^{*2}\omega} \sum_{n,m,k_z,n'} \left| \int_{r_a}^{r_b} rdr \left[B_1 J_{v_\pm}(k'r) + B_2 N_{v_\pm}(k'r)\right]\left\{-B_1\frac{\partial J_v(kr)}{\partial r} - B_2\frac{\partial N_v(kr)}{\partial r}\right.\right.$$
$$\left.\left. \mp \frac{m}{r}[B_1 J_v(kr) + B_2 N_v(kr)] \pm \frac{bk_z}{2\pi r}[B_1 J_v(kr) + B_2 N_v(kr)]\right\}\right|^2 \delta\left(E_{v,k,k_z}\right.$$
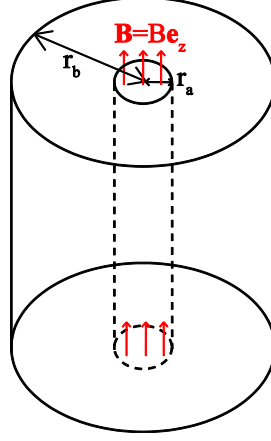$$\left. - E_{v_\pm,k',k_z} - \hbar\omega\right), \tag{30}$$

where

Fig. 2 Schematic view of the three-dimensional system with magnetic field $\boldsymbol{B} = B\boldsymbol{e}_z$ in the hollow region

$$\nu_{\pm} = \sqrt{\left(m \pm 1 + \frac{k_z b}{2\pi}\right)^2 + \frac{b^2}{2\pi^2 a^2}\left(1 - \frac{k_z{}^2 a^2}{2}\right)} \tag{31}$$

has a double sign of the same order. Numerical integration is performed to calculate $\sigma(\omega)$ in Eq. (30) whose results will be given in Section 4.

To extract the differences in AC conductivity between the screw-dislocated system and the AB system, we also calculate the AC conductivity of the AB system shown in Fig. 2. Electrons are restricted to moving in a region bounded by the cylindrical surfaces $r = r_a$ and $r = r_b$ with $r_b > r_a$. The magnetic field $\boldsymbol{B} = B\boldsymbol{e}_z$ penetrates the region of $r < r_a$ in the z-direction and a magnetic flux Φ is given by $\Phi = \pi r_a{}^2 B$. A mathematical expression of the AC conductivity of the AB system is found by replacing $\pm b k_z/(2\pi r)$ in Eq. (30) by $\pm \Phi/\Phi_0$ and $\nu_{\pm}$ in Eq. (31) by $m \pm 1 + \Phi/\Phi_0$, where Φ_0 is a flux quantum $2\pi\hbar/e$.

4. Results and discussion

4.1 Setting parameters for numerical calculations

From the viewpoint of experimental realization, we set parameters using SiC as a reference, snce it is a promising material for high temperature, high power, and/or high frequency applications (Nieberding 1983, Parsons *et al.* 1985, Segall *et al.* 1986, Agueev *et al.* 2000, Asada and Suzuki 2011). However, since screw dislocations observed in the SiC (Vetter and Dudley 2004) depress device performance, Berechman *et al.* (2010), Chung *et al.* (2011) and Sugawara *et al.* (2012) investigated the influences of screw dislocation on electronic states. Taking their results into consideration, the lattice constant and the effective mass are set to $a = 4.4$ Å and $m^* = 0.68 m_0$, respectively, where m_0 is the mass of a free electron. The amplitude of the Burgers vec-

tor and the inner and outer radii of the cylinder are set to $b/a = 1$, $r_a = 0.1$ μm and $r_b = 0.2$ μm, respectively.

4.2 Numerical results

Fig. 3 shows a plot of the AC conductivity $\sigma(\omega)$ as a function of the angular frequency ω. E_F is set to (a) 5 meV and (b) 10 meV. $\sigma(\omega)$ is numerically obtained by using Eq. (30), in which the wave functions given by Eqs. (22)-(25) are substituted. The most important observation is that the amplitude of $\sigma(\omega)$ in the case of $b/a = 1$ (red line) is much larger than that of $b/a = 0$ (not shown since it lies on $\sigma(\omega) = 0$) in both (a) $E_F = 5$ meV and (b) $E_F = 10$ meV. This result means that the screw dislocation enhances the amplitude of $\sigma(\omega)$ over the whole frequency range in the THz order and its value of several μS/m is measurable experimentally (Kitao 1972, Mirsaneh *et al.* 2010, Asada and Suzuki 2011).

The effects of screw dislocation can also be measured by the increase in the amplitude and the occurrence of an additional peak when the Fermi energy E_F is changed. The amplitude of $\sigma(\omega)$ in the case of $E_F = 10$ meV is almost double compared to that of $E_F = 5$ meV. This is because, generally, the double E_F increases the number of degenerate energy levels, and thus, the number of electrons contributing to $\sigma(\omega)$ increases (see Fig. 4). Therefore, doubling E_F induces the amplitude of $\sigma(\omega)$ to double. A qualitative difference in $\sigma(\omega)$ between $E_F = 10$ meV and $E_F = 5$ meV is seen in the additional peak that appears at about $\omega = 0.52$ THz when $E_F = 10$ meV. This additional peak is originated by the excitation of electrons lying on the energy ΔE between $E_F = 10$ meV and $E_F = 5$ meV (see Fig. 5). The necessary condition of this pumping is that the AC field energy $\hbar\omega = (1.06 \times 10^{-34}) \times (0.52 \times 10^{12}) \sim 0.1$ meV matches the energy difference between ΔE and the energy higher than $E_F = 10$ meV. This condition is satisfied in the case of $E_F = 10$ meV, which is why the additional peak appears at $\omega = 0.52$ THz. Whereas, in the case of $E_F = 5$ meV, electrons do not absorb the energy of the AC field since $\hbar\omega = 0.1$ meV matches the electrons' forbidden band and thus the peak at $\omega = 0.52$ THz does not appear.
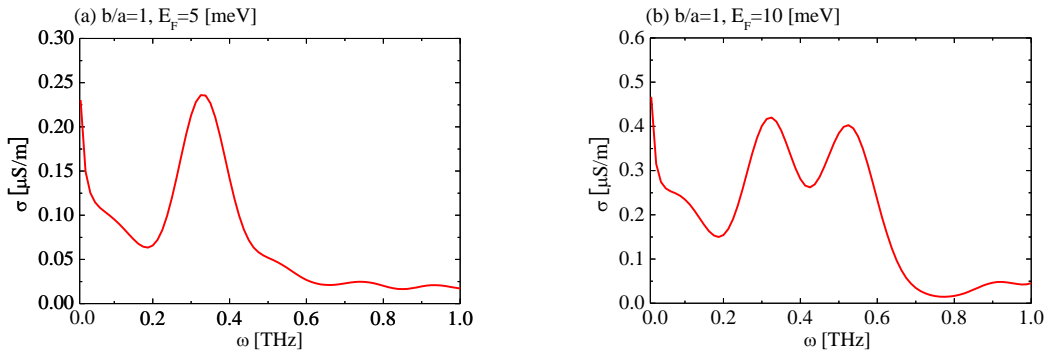

Fig. 3 Alternating current conductivity $\sigma(\omega)$ as a function of the angular frequency ω. The amplitude of the Burgers vector and the Femi energy are set to $b/a = 1$ and (a) $E_F = 5$ meV, (b) $E_F = 10$ meV, respectively
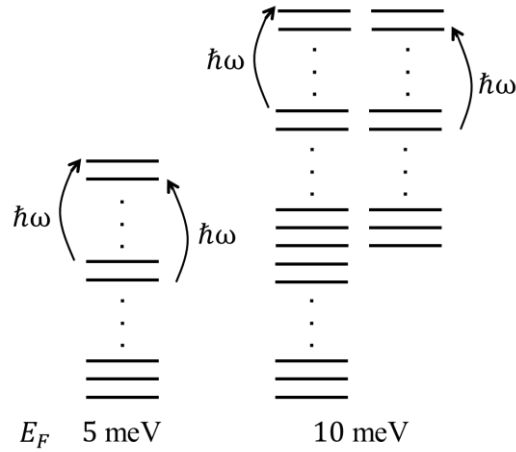
Fig. 4 An example of the energy level of electrons. In this example, the energy does not degenerate in the case of $E_F = 5$ meV, but doubly degenerate in the case of $E_F = 10$ meV
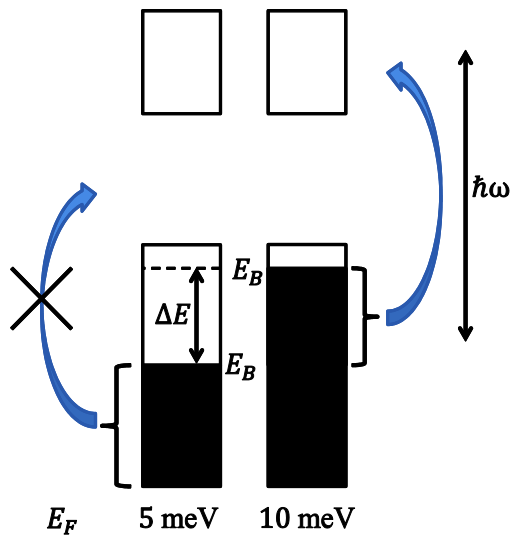

Fig. 5 Schematic illustration of the band structure of electrons. Black and white areas show occupied and unoccupied energy levels, respectively. Electrons do not absorb the energy $\hbar\omega$ of the alternating current field in the case of $E_F = 5$ meV. In the case of $E_F = 10$ meV, electrons lying on the energy ΔE are excited by absorbing the energy $\hbar\omega$

In order to promote a deeper understanding of the characteristics of $\sigma(\omega)$ enhanced by the Burgers vector, we plotted $\sigma(\omega)$ in the AB system. Figure 6 shows the same plot as Fig. 3 but b/a is replaced by Φ/Φ_0. The amplitude of the flux is set to $\Phi/\Phi_0 = 0.01$ since this value is comparable to $bk_z/(2\pi a) = 1$. It can be seen that $\sigma(\omega)$ in both the screw-dislocated system and the AB system exhibit the same function form. This means that we cannot recognize the qualitative
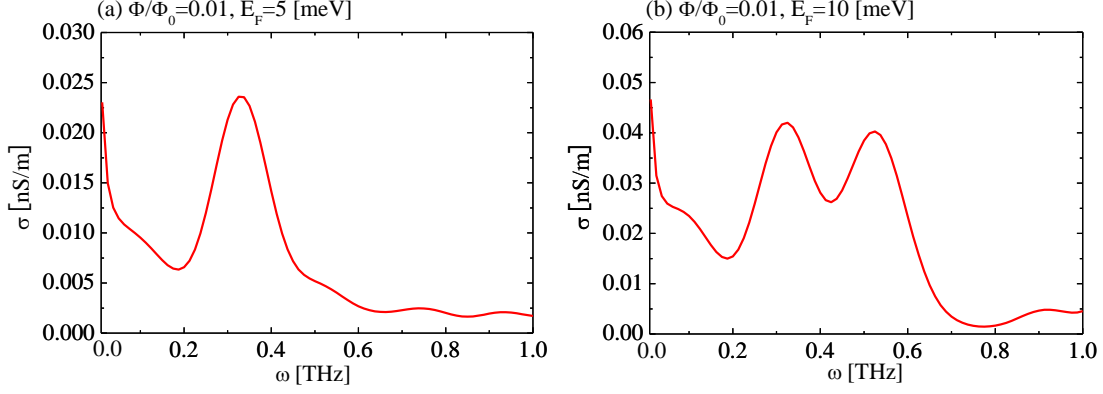
Fig. 6 Same as Fig. 3, but b/a is replaced by Φ/Φ_0. The amplitude of the flux is set to $\Phi/\Phi_0 = 0.01$

difference between them. However, the main feature is that the quantitative difference is remarkable, that is, the amplitude of $\sigma(\omega)$ in the screw-dislocated system is 10^4 times larger than in the AB system. Furthermore, several nS/m of $\sigma(\omega)$ in the case of the AB system are not measurable experimentally. Therefore, it should be noted again that $\sigma(\omega)$ in the screw-dislocated system is large enough to measure, but is too small to measure in the AB system. This difference in behaviour originates from the different contribution of the effective vector potential $\boldsymbol{A}^{\text{eff}}$ and the vector potential $\boldsymbol{A}$. That is, the difference between $\boldsymbol{A}^{\text{eff}}$ and $\boldsymbol{A}$ is the effective vector potential part of the current operator given in Eq. (29). This part is expressed by $m - bk_z/(2\pi)$ for the screw-dislocated system and $m - \Phi/\Phi_0$ for the AB system. Thus, $\sigma(\omega)$, in the case of the screw- dislocated system, becomes large since the $bk_z/(2\pi)$ part contributes to the sum of k_z in Eq. (30) and its contribution makes $\sigma(\omega)$ increase owing to the absolute value on the right side of the equation.

4.2 Discussion

Our calculations are based on Eq. (30) with the wave functions given in Eqs. (22)-(25), which are obtained by the approximation of short wave length $kr_a \gg 1$ and $kr_b \gg 1$. Therefore, the sum of n in Eq. (30) is also taken only large value. This indicates that our current evaluations are not sufficient to accurately predict the function form of $\sigma(\omega)$. To improve on this, the exact solution would be used to calculate $\sigma(\omega)$ in Eq. (30). The exact solution is derived by solving the secular equation given in Eq. (21). Since exact wave functions take all wave numbers, the sum of n in Eq. (30) also takes on a large value. Therefore, a more accurate function form of $\sigma(\omega)$ will be able to be found in future studies.

5. Conclusions

We numerically calculated the alternating current (AC) conductivity of a simple cubic crystal

with a single hollow screw dislocation and of the AB system for comparison. The amplitude of the conductivity in the case of the screw-dislocated system shows a sufficiently large value for experimental measurements, whereas that of the AB system is not measurable due to its small value, despite both systems having similar electronic eigenstates. The difference in AC conductivity is caused by the current operator in the Kubo formula. The current operator depends on k_z for the screw-dislocated system but does not depend on k_z for the AB system, thus, the AC conductivity behaves in a different manner in each system since the sum of k_z has to be taken.

Acknowledgments

References

Agueev, O., Svetlichny, A.M., Izotovs, D.A., Melnikov, A.V. and Voronko, A.B. (2000), "Temperature dependence simulation of electrophysical properties of silicon carbide", *ASDAM2000 Conf. Proc.*, 295-298.

Aharonov, Y. and Bohm, D. (1959), "Significance of electromagnetic potentials in the quantum theory", *Phys. Rev.*, **115**(3), 485-491.

Araki, H., Kitahara, K. and Nakazato, K. (1981), "Riemannian-geometrical interpretation of quantum motion of a particle in a dislocated crystal", *Prog. Theor. Phys.*, **66**(5), 1895-1898.

Asada, M. and Suzuki, S. (2011), "Terahertz oscillators using electron devices – an approach with resonant tunneling diodes", *IEICE Electr. Exprs.*, **8**(14), 1110-1126.

Azevedo, S. and Moraes, F. (1998), "Topological Aharonov-Bohm effect around a disclination", *Phys. Lett. A*, **246**(4-6), 374-376.

Azevedo, S. and Pereira, J. (2000), "Double Aharonov-Bohm effect in a medium with a disclination", *Phys. Lett. A*, **275**(5-6), 463-466.

Bakke, K. and Moraes, F. (2012), "Threading dislocation densities in semiconductor crystals: a geometrical approach", *Phys. Lett. A*, **376**(45), 2838-2841.

Bausch, R., Schmitz, R. and Turski, L.A. (1998), "Single-particle quantum states in a crystal with topological defects", *Phys. Rev. Lett.*, **80**(11), 2257-2260.

Bausch, R., Schmitz, R. and Turski, L.A. (1999a), "Quantum motion of electrons in topologically distorted crystals", *Ann. Phys. (Leipzig)*, **8**(3), 181-189.

Bausch, R., Schmitz, R. and Turski, L.A. (1999b), "Scattering of electrons on screw dislocations", *Phys. Rev. B*, **59**(21), 13491-13493.

Berechman, R.A., Skowronski, M., Soloviev, S. and Sandvik, P. (2010), "Electrical characterization of 4H-SiC avalanche photodiodes containing threading edge and screw dislocations", *J. Appl. Phys.*, **107**(111), 114504:1-114504:4.

Bilby, B.A., Bullough, R. and Smith, E. (1955), "Continuous distribution of dislocations: a new application of the methods of non-Riemannian geometry", *Proc. R. Soc. London A*, **231**, 263-273.

Carvalho, A.M. de M., Sátiro, C. and Moraes, F. (2007), "Aharonov-Bohm-like effect for light propagating in nematics with disclinations", *Eur. Phys. Lett.*, **80**(4), 46002:1-46002:6.

Chung, S., Berechman, R.A., McCartney, M.R. and Skowronski, M. (2011), "Electronic structure analysis of

threading screw dislocations in 4H-SiC using electron holography", *J. Appl. Phys.*, **109**(3), 034906:1-034906:6.

Dudley, M., Huang, X.R. and Vetter, W.M. (2003), "Contribution of x-ray topography and high-resolution diffraction to the study of defects in SiC", *J. Phys. D: Appl. Phys.*, **36**(10A), A30-A36.

Dumiszewska, E., Strupinski, W. and Zdunek, K. (2007), "Interaction between dislocations density and carrier concentration of gallium nitride layers", *J. Superhard Mater.*, **29**(3), 174-176.

Furtado, C., Bezerra, V.B and Moraes, F. (2001), "Quantum scattering of by a magnetic flux screw dislocation", *Phys. Lett. A*, **289**(3), 160-166.

Gilbert, M.R., Queyreau, S. and Marian, J. (2011), "Stress and temperature dependence of screw dislocation mobility in α-Fe by molecular dynamics", *Phys. Rev. B*, **84**(17), 174103:1-174103:11.

Kawamura, K. (1978), "A new theory on scattering of electrons due to spiral dislocations", *Z. Physik B*, **29**(2), 101-106.

Kitao, M. (1972), "Ac conductivity of amorphous As_2Se_3'', *Jpn. J. Appl. Phys.*, **11**(10), 1472-1479.

Kubo, R. (1957), "Statistical mechanical theory of irreversible processes. I. general theory and simple applications to magnetic and conduction problems", *J. Phys. Soc. Jpn.*, **12**(6), 570-586.

Look, D.C. and Sizelove, J.R. (1999), "Dislocation scattering in GaN", *Phys. Rev. Lett.*, **82**(6), 1237-1240.

Ma, X. (2006), "A method to determine superscrew dislocation structure in silicon carbide", *Mater. Sci. Eng. B*, **129**(1-3), 216-221.

Mirsaneh, M., Furman, E., Ryan, J.P., Lanagan, M.T. and Pantano, C.G. (2010), "Frequency dependent electrical measurements of amorphous GeSbSe chalcogenide thin films", *Appl. Phys. Lett.*, **96**(11), 112907:1-112907:3.

Netto, A.L.S. and Furtado, C. (2008), "Elastic landau levels", *J. Phys.: Condens. Matter.*, **20**(19), 15209:1-15209:9.

Nieberding, W.C. (1983), "Researchers develop long-sought SiC crystal growth techniques", *Ind. Res. Dev.* **25**, 148-150.

Parsons, J.D., Bunshah, R.F. and Stafsudd, O.M. (1985), "Unlocking the potential of beta silicon carbide", *Solid State Technol.*, **28**(11), 133-139.

Schafler, E., Zehetbauer, M. and Ungár, T. (2001), "Measurement of screw and edge dislocation density by means of X-ray Bragg profile analysis", *Mater. Sci. Eng. A*, **319-321**, 220-223.

Segall, B., Alterovitz, S.A., Haugland, E.J. and Matus, L.G. (1986), "Compensation in epitaxial cubic SiC films", *Appl. Phys. Lett.*, **49**(10), 584-586.

Si, W., Dudley, M., Glass, R. Tsvetkov, V. and Carter, C. Jr. (1997), "Hollow-core screw dislocations in 6H-SiC single crystals: a test of Frank's theory", *J. Elect. Mater.*, **26**(3), 128-133.

Sugawara, Y., Nakamori, M., Yao, Y.Z., Ishikawa, Y., Danno, K., Suzuki, H., Bessho, T., Yamaguchi, S., Nishikawa, K. and Ikuhara, Y. (2012), "Transmission electron microscopy analysis of a threading dislocation with c+a Burgers vector in 4H-SiC", *Appl. Phys. Exp.*, **5**(8), 081301:1-081301:3.

Turski, L.A., Bausch, R. and Schmitz, R. (2007), "Gauge theory of sound propagation in crystals with dislocations", *J. Phys.: Condens. Matter.*, **19**(9), 096211:1-096211:6.

Turski, L.A. and Mińkowski, M. (2009), "Spin wave interaction with topological defects", *J. Phys: Condens. Matter.*, **21**(37), 376001:1-376001:4.

Vetter, W.M. and Dudley, M. (2002), "Surface-relaxation contributions to axial screw dislocation contrast in synchrotron white-beam X-ray topographs of SiC", *J. Appl. Cryst.*, **35**(6), 689-695.

Vetter, W.M. and Dudley, M. (2004), "Micropipes and the closure of axial screw dislocation cores in silicon carbide crystals", *J. Appl. Phys.*, **96**(1), 348-353.

CC